Plant Pathol. J. 40(5) : 438-450 (2024)
https://doi.org/10.5423/PPJ.OA.07.2024.0107
eISSN 2093-9280

Research Article Open Access

The Plant Pathology Journal

Arabidopsis MORC1 and MED9 Interact to Regulate Defense Gene Expression and Plant Fitness

Ji Chul Nam, Padam Shekhar Bhatt, April Bonnard‡, Dinesh Pujara, and Hong-Gu Kang *

Department of Biology, Texas State University, 600 University Dr., San Marcos, TX 78666, USA
‡Current address: Rules Based Medicine, Austin, TX 78759, USA

(Received on July 22, 2024; Revised on August 9, 2024; Accepted on August 11, 2024)

Arabidopsis MORC1 (Microrchidia) is required for multiple levels of immunity. We identified 14 MORC1-interacting proteins (MIPs) via yeast two-hybrid screening, eight of which have confirmed or putative nuclear-associated functions. While a few MIP mutants displayed altered bacterial resistance, MIP13 was unusual. The MIP13 mutant was susceptible to *Pseudomonas syringae*, but when combined with *morc1/2*, it regained wild-type resistance; notably, *morc1/2* is susceptible to the same pathogen. MIP13 encodes MED9, a mediator complex component that interfaces with RNA polymerase II and transcription factors. Expression analysis of defense genes *PR1*, *PR2*, and *PR5* in response to avirulent *P. syringae* revealed that *morc1/2 med9* expressed these genes in a slow but sustained manner, unlike its lower-order mutants. This expression pattern may explain the restored resistance and suggests that the interplay of MORC1/2 and MED9 might be important in curbing defense responses to maintain fitness. Indeed, repeated challenges with avirulent *P. syringae* triggered significant growth inhibition in *morc1/2 med9*, indicating that MED9 and MORC1 may play an important role in balancing defense and growth. Furthermore, the *in planta* interaction of MED9 and MORC1 occurred 24 h, not 6 h, post-infection, suggesting that the interaction functions late in the defense signaling. Our study reveals a complex interplay between MORC1 and MED9 in maintaining an optimal balance between defense and growth in Arabidopsis.

Keywords **:** Arabidopsis, defense, growth, mediator, MORC1

*Corresponding author.
Phone) +1-512-245-7508, FAX) +1-512-245-8713
E-mail) kang@txstate.edu
ORCID
Hong-Gu Kang
https://orcid.org/0000-0002-5842-8945

Handling Editor : Hee Jin Park

Plants have evolved an innate immune system against pathogens (Chisholm et al., 2006; Jones and Dangl, 2006). The perception of pathogen-associated molecular patterns (PAMPs) initiates the first line of defense, PAMP-triggered immunity (PTI) (Jones and Dangl, 2006; Zipfel and Felix, 2005). To counteract PTI, pathogens secrete effectors, leading to effector-triggered susceptibility. In response, plants have developed effector-triggered immunity (ETI), where resistance (R) proteins recognize effectors, triggering a stronger defense response (Chisholm et al., 2006; Jones and Dangl, 2006). ETI involves programmed cell death (hypersensitive response), calcium flux, oxidative burst, and transcriptional reprogramming (Hammond-Kosack and Jones, 1996). Many R proteins contain nucleotide-binding sites and leucine-rich repeats domains (Chisholm et al., 2006). Although ETI is stronger than PTI, the difference is mostly quantitative, involving similar defense genes (Tao et al., 2003; Tsuda et al., 2009), suggesting that R proteins amplify common defense signaling in ETI and PTI upon effector recognition (Ngou et al., 2021).

Most ecotypes of Arabidopsis are susceptible to *Turnip crinkle virus* (TCV) except for Di-17 (Dempsey et al., 1997). CRT1 (Compromised Recognition to TCV-CP 1) was identified in a screen for mutants that fail to

develop hypersensitive response against the coat protein of TCV (Kang et al., 2008). It was later renamed MORC1 as it belongs to the microrchidia (MORC) protein family (Koch et al., 2017). MORC1 and its homolog, MORC6, are required for epigenetic gene silencing, as evidenced by the de-repression of silenced reporter genes and transposable elements (TEs) in *morc1* and *morc6* mutants (Brabbs et al., 2013; Lorkovic et al., 2012; Moissiard et al., 2012). MORC1 and its closest homolog, MORC2, are essential for PTI, ETI, basal resistance, non-host resistance, and systemic acquired resistance (Kang et al., 2008, 2010, 2012). MORC1 physically associates with numerous immune components, including at least 12 R proteins and the PAMP recognition receptor FLS2. Intriguingly, MORC1 increases in the nucleus upon the activation of PTI and ETI, suggesting that its nuclear function may be crucial in defense responses (Kang et al., 2012).

MORC proteins are chromatin remodeling factors, and contain GHKL ATPase and CW histone recognition domains (Hoppmann et al., 2011; Iyer et al., 2008). They bind nucleic acids and exhibit Mn^{2+}-dependent endonuclease and ATPase activity (Kang et al., 2008, 2012). MORC proteins regulate chromatin compaction and directly compact DNA (Kim et al., 2019), essential for heterochromatin maintenance. This topology-associated function explains MORC1's role in suppressing hypermethylated genes and TEs (Moissiard et al., 2012) and modulating physical accessibility to TEs near defense-related genes (Bordiya et al., 2016). However, the timing and mechanism of this physical topology's importance in defense genes remains unknown.

The mediator (MED) complex, a large and multi-subunit RNA polymerase II-associated transcriptional regulator, coordinates various aspects of transcription and acts as a docking site for nuclear machinery (An and Mou, 2013; Buendía-Monreal and Gillmor, 2016; Conaway and Conaway, 2011; Kelleher et al., 1990; Samanta and Thakur, 2015a). It consists of four distinct modules: head, middle, tail, and cyclin-dependent kinase, each with specific roles in transcriptional regulation. In Arabidopsis, the MED complex is involved in the development and modulation of biotic and abiotic stresses (Malik et al., 2017). Extensive evidence demonstrates its importance in plant resistance to various pathogens, with genetic mutants of MED subunits displaying altered resistance and changes in defense-related genes. Examples include MED5a/b in phenylpropanoid pathways (Bonawitz et al., 2014), MED8 in jasmonic acid (JA) and salicylic acid (SA)-dependent defense (Kidd et al., 2011; Zhang et al., 2012), MED14 and MED15 in SA-induced resistance (Zhang et al., 2013), MED16 in basal resistance (Wang et al., 2015), MED18 in JA/ethylene (ET) signaling (Fallath et al., 2017), MED19 in JA-responsive genes (Caillaud et al., 2013), MED21 in susceptibility to necrotrophic fungi (Dhawan et al., 2009), and MED25 in JA-responsive defense and herbivore genes (Chen et al., 2012; Kidd et al., 2009). These findings highlight the role of the MED complex in coordinating transcription factors and RNA polymerase II during the massive transcriptional reprogramming required for plant defense responses (An and Mou, 2013; Yang et al., 2016).

Mounting a defense response comes with a fitness cost, which often manifests as a reduction in growth and reproduction. This trade-off carries critical implications for agricultural populations (Karasov et al., 2017). Intriguingly, growth-defense trade-offs can be decoupled under specific conditions, suggesting that the fitness cost can be minimized while maintaining adequate defense responses (Burdon and Thrall, 2003; Campos et al., 2016; van Hulten et al., 2006). Hormones such as gibberellins, SA, and JA play crucial roles in modulating the growth-immunity balance (Daviere and Achard, 2013; Gangappa et al., 2017; Navarro et al., 2008; Sun et al., 2011; Wang et al., 2015). Given the involvement of chromatin remodeling factors and transcriptional regulators in plant defense responses, it is plausible that these components also contribute to balancing growth and immunity.

In this study, we searched for MORC1 interacting proteins (MIPs) and further focused on one: MED9, a subunit of the MED complex, because of the unexpected disease resistance phenotypes of the combined mutant, *morc1/2 med9*. We attribute this unexpected gain of resistance to the inability to curb defense responses when MORC1 and MED9 are compromised. The physical interaction between MORC1 and MED9 observed at later stages of infection is also in line with this hypothesis, suggesting that the MORC1 and MED9 interaction is likely important in balancing defense and growth responses in Arabidopsis.

Materials and Methods

DNA constructs. The yeast two-hybrid constructs received from Hybrigenics Services (Evry-Courcouronne, France) were used to switch the prey and the bait clones by using *SfiI* restriction sites to validate the MORC1-MIP interaction. Genomic MED9 amplified from BAC T7N22 was digested with *XhoI* and ligated into the pBKS plasmid to generate pBKS-gMED9. A Flag-tag was introduced into pBKS-gMED9 using Cas9 Nuclease from New England Biolabs (NEB, Ipswhich, MA, USA) to create pBSK-gMED9-Flag. The gMED9-Flag fragment was then ex-

cised using *XhoI* and ligated into the pPZP-RCS2-hptII vector using *SalI* to generate pPZP-gMED9-Flag. The pER8-Myc-MORC1 construct was described previously (Kang et al., 2012). The coding sequence of the *MIP* genes were cloned into pER8 tagged at the 3′ end with triple HA (pET-HA) by using *Asc*I sites and transformed into *Agrobacterium tumefaciens* strain GV2260 using electroporation.

Yeast two-hybrids. pB27 bait and pP6 prey plasmids were transformed into Y187 and L40 yeast strains, respectively. This yeast two-hybrid system uses the *HIS3* reporter gene, which encodes imidazoleglycerol-phosphate dehydratase, an enzyme required for the synthesis of the amino acid histidine (His). In the yeast two-hybrid system, the interaction between the bait and prey proteins leads to the reconstitution of a functional transcription factor, which activates the expression of the *HIS3* reporter gene. Minimal media containing His was used to demonstrate growth, while media lacking His was used to test the interaction between the prey and bait proteins. A competitive inhibitor of His synthesis, 3-amino-1,2,4-triazole (3-AT), was used to evaluate the strength of the interaction. A stronger interaction leads to higher *HIS3* expression, which can outcompete 3-AT. A concentration of 0.1 mM 3-AT was used to create a stringent condition for selecting strong interactions.

Transient expression in *Nicotiana benthamiana*. The growing of the Agrobacterium culture and its infiltration process were performed as described (Menke et al., 2005). pBA-HcPro was used to suppress gene silencing to maximize the transient expression. A solution of 30 μM estradiol in 0.1% Tween-20 was sprayed on the leaves to induce the expression of pER8-based constructs at 1-day post-infiltration. These plants were then grown for an additional 2 days at room temperature.

Immunoblotting analysis. Immunoblotting analysis was performed as described using an enhanced chemiluminescence method (Kang and Klessig, 2005). Tissue samples in 2 ml tubes were ground with a ceramic bead with 4× sodium dodecyl sulfate (SDS) sample buffer containing dithiothreitol (DTT) at 60 mg/ml using a homogenizer. Once homogenized, these samples were boiled for 5 min and centrifuged at 21,100 ×*g* for 1 min. Five microliters of supernatant was loaded into sodium dodecyl sulfate polyacrylamide gel electrophoresis and transferred onto a polyvinylidene difluoride membrane (Immobilon, Millipore, Billerica, MA, USA) using a standard transfer buffer. The rest of the immunoblotting analysis was performed as previously described (Kang and Klessig, 2005) with the following differences: ECL2 solution (Thermo Fisher Scientific, Waltham, MA, USA) was used to detect the antibodies, and the membrane was imaged using an Azure Biosystems C600 imager (Dublin, CA, USA). Antibodies used include HRP-conjugated anti-Myc (1:5,000, Santa Cruz Biotechnology, Santa Cruz, CA, USA), HRP-conjugated anti-FLAG (1:5,000, Sigma, St. Louis, MO, USA), and HRP-conjugated anti-HA (1:10,000, Sigma).

Co-immunoprecipitation. Leaves of Arabidopsis or *N. benthamiana* were homogenized with a mortar and pestle in liquid nitrogen. Samples were ground again in 750 μl of extraction buffer (GTEN buffer: 150 mM NaCl, 1 mM EDTA, 25 mM Tris pH 7.5, and 10% glycerol) with 2% polyvinylpolypyrrolidone, 1× protease inhibitor cocktail (Sigma), and 0.1% Triton X-100. These protein extracts were collected and centrifuged at 5,000 ×*g* at 4°C for 5 min, and 0.5 ml of the supernatant was then subjected to size exclusion chromatography using Illustra NAP-5 Sephadex G-25 DNA grade columns (GE Healthcare, Pittsburgh, PA, USA) to remove salts and perform buffer exchange. Eluates were collected in 1.5 ml tubes, mixed with 20 μl of anti-mouse IgG agarose beads (Sigma), and incubated at 4°C for 2 h with gentle rotation. After removing the anti-mouse IgG agarose beads, the remaining solutions were mixed with 20 μl of agarose beads conjugated with a target antibody and incubated at 4°C overnight. These solutions were washed a minimum of six times with 1 ml of IP buffer (GTEN buffer with 0.15% NP-40 and 5 mM DTT) and mixed with 30 μl of 4× SDS sample buffer before proceeding to immunoblotting analysis.

Imaging-based and conventional leaf-disc-based resistance assay. Three point five-week-old Arabidopsis plants were syringe-infiltrated with an indicated inoculum of *Pseudomonas syringae* pv. *tomato DC3000* (*Pst*) grown for 2 days at 28°C in King's B medium with appropriate antibiotics. Imaging-based resistance assays were performed as previously described (Pujara et al., 2021) except that *Pst* carrying the *luxCDABE* operon was used.

For a conventional leaf-disc-based resistance assay in Arabidopsis, three leaf disks were collected into a single 2 ml tube and homogenized using a homogenizer for 1 min in 500 μl of 0.01% Triton X-100. The samples were incubated on a mild rotating shaker for 10 min and then homogenized again in the shaker for 1 min. Samples were vortexed briefly and serially diluted. Twenty microliters of all dilutions were then plated on Luria-Bertani, and colonies were counted after 36 h.

Fitness cost test. Three point five weeks after germination, two leaves from each plant were infected with *Pst* carrying *AvrRpt2* at 1×10^5 cfu/ml every 2 days for 3 weeks. Upon completion of the treatment, plants were imaged to check the growth and development characteristics.

RNA preparation, cDNA synthesis, and quantitative reverse transcription PCR analysis. Two leaves were generally collected in a single tube and homogenized in a shaker for 1 min using a bead. Their RNA was extracted using the Purelink RNA Mini kit 250 (Thermo Fisher Scientific). For quantification, RNA was converted to cDNA using SuperScript RT (Invitrogen, Carlsbad, CA, USA). The primers used in reverse transcription PCR are as follows: PR1-For (AAAACTTAGCCTGGGGTAGCGG), PR1-Rev (CCACCATTGTTACACCTCACTTT), PR2-For (ATCAAGGAGCTTAGCCTCAC), PR2-Rev (TGTAAAGAGCCACAACGTCC), PR5-For (CTCTTCCTCGTGTTCACTCAC), PR5-Rev (GAAGCACCTGGAGTCAATTC), Tip41-Like-For (GCGATTTTGGCTGAGAGTTGAT), and Tip41-Like-Rev (GGATACCCTTTCGCAGATAGAGAC). Maxima SYBR Green qPCR Master Mix (Thermo Fisher Scientific) was used for quantitative reverse transcription PCR (qRT-PCR). PCR was performed with the following temperature/time profile: 50°C for 2 min and 95°C for 10 min, followed by 40 cycles of 95°C for 25 s and 60°C for 1 min.

Genetic resources. Generation of *Myc-gCRT1* transgenic line is as described (Kang et al., 2012). *med9* was tranformed with pPZP-gMED9-Flag and subsequentely crossed with *Myc-gCRT1* line to generate *Myc-gCRT1 gMED9-Flag* in *morc1/2 med9*. The following mutant lines were obtained from The Arabidopsis Information Resource (TAIR): *cpl3* (c-terminal phosphatase-like3, *med4*), SALK 051322; GNARLED (*med5*), SALK 014298; *smc1* (structural maintenance of chromosomes1, *mip8*), CS87452; a trihelix transcription factor (*mip9*), SALK 024424; *bzip29* (basic leucine zipper29, *mip10*), SALK 018426; a mobile domain protein (*med12*), SALK 066042; *med9* (*med13*), SALK 029120.

Plants growth. Plants were grown in soil in a growth chamber under long-day photoperiod (16 h light, 12k lux of cool white fluorescence bulbs) at 23°C, 60% relative humidity.

Results

A yeast two-hybrid screening identified 14 MORC1 interaction proteins. A conventional yeast two-hybrid (Y2H) screening for MORC1 as a bait was performed by Hybrigenics using 87 million prey clones. The commercial service provided 14 confirmed clones that interacted with the bait, which are listed in Table 1. To validate the physical interaction between MORC1 and its interacting proteins, MIPs, we generated a targeted Y2H assay with the bait and prey vectors for MORC1 and all 14 MIPs, respectively

Table 1. MORC1 interacting protein (MIP) identified in the yeast two-hybrid screening

	Locus	Annotated name	Reference
MIP1	At3g56190	α Soluble NSF attachment protein 2 (SNAP2)	-
MIP2	At5g15450	Albino and pale green 6 (APG6)	-
MIP3	At1g19100	MORC6	Moissiard et al. (2014)
MIP4	At2g33540	C-terminal domain phosphatase-Like3 (CPL3)	Li et al. (2014)
MIP5	At2g35110	GNARLED	Gieni et al. (2009)
MIP6	At5g51600	Microtubule-associated protein 65-3 (MAP65-3)	-
MIP7	At4g27500	Proton pump interactor 1 (PPI1)	-
MIP8	At3g54670	Structural maintenance of chromosomes 1 (SMC1)	Wood et al. (2010)
MIP9	At3g10030	A trihelix transcription factor	Boyer et al. (2004)
MIP10	At4g38900	Basic leucine-zipper29 (BZIP29)	Dröge-Laser et al. (2018)
MIP11	At5g06140	Sorting nexin 1 (SNX1)	-
MIP12	At1g50750	A mobile domain protein	Nicolau et al. (2020)
MIP13	At1g55080	Mediator 9 (Med9)	Zhu et al. (2011)
MIP14	At1g31780	Conserved oligomeric complex (COG6)	-

The annotation and locus of 14 MIPs were based on The Arabidopsis Information Resource. References are listed for eight MIPs with a putative nuclear-associated function.

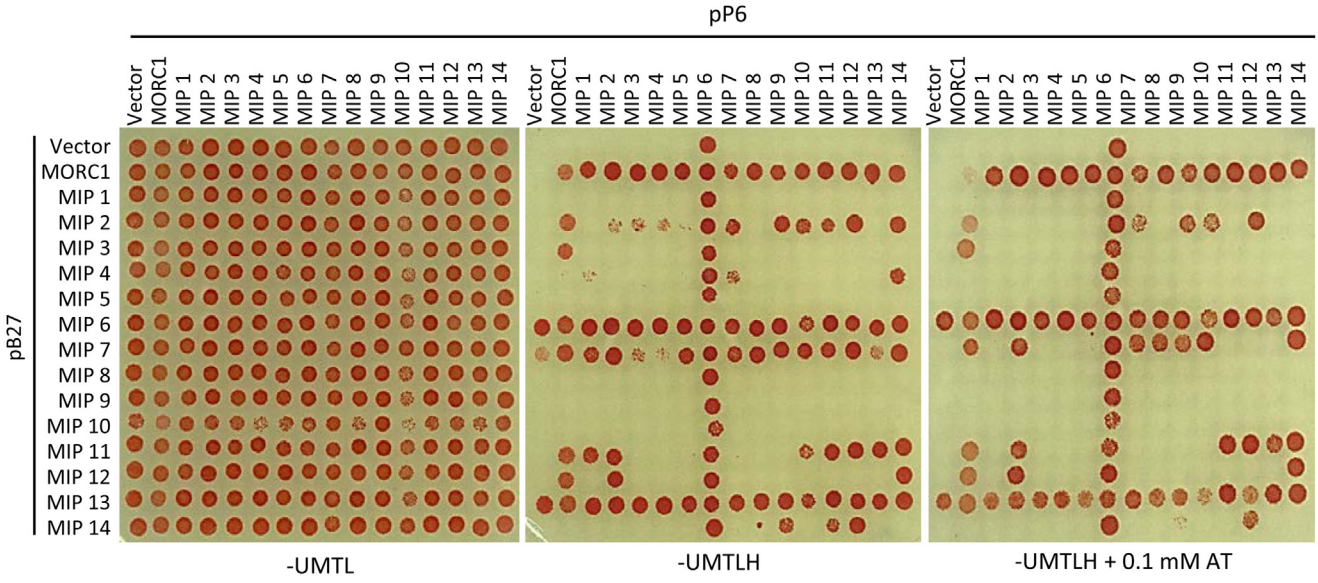

Fig. 1. Verification of the interaction between MORC1 and its interacting proteins in yeast two-hybrid assay. MORC1 and 14 MORC1-interacting protein (MIP) clones identified from the yeast two-hybrid screening were reconfirmed by a targeted yeast two-hybrid assay. pB27 plasmid with a LexA DNA binding domain (Y187) and pP6 plasmid with a GAL4 activating domain (L40) were used as a bait and a prey vector, respectively. The plasmids were transformed into *S. cerevisiae* carrying the *HIS3* reporter gene under the control of the *LexA* DNA binding sites. Transformants were plated onto minimal media lacking uracil, methionine, tryptophan, and leucine (-UMTL) or lacking uracil, methionine, tryptophan, leucine, and histidine (-UMTLH), with or without 0.1 mM 3-amino-1,2,4-triazole (3-AT), a competitive inhibitor of the *HIS3* gene product.

(Fig. 1). In addition, we also generated constructs that switched the bait and the prey. MORC1, when used as bait, interacted with all the MIP clones identified in the screen, confirming the outcome provided by Hybrigenics, while MIP6 displayed autoactivation. MORC1 showed a weak interaction with itself, suggesting homodimerization. When MORC1 was switched to prey (pP6-MORC1), it interacted with a subset of the MIPs: MIP2, MIP3, MIP7, MIP11, and MIP12 (Fig. 1). When a transcription-activating domain is present in a bait vector, it generally activates without a prey vector. This transactivation was observed with MIP6 and MIP13, and to a lesser degree, with MIP7, suggesting that these MIP proteins may carry a transactivation domain. As previously stated, MIP13 (MED9) is part of the MED complex that interfaces a transcription factor with RNA polymerase II (Allen and Taatjes, 2015; Buendía-Monreal and Gillmor, 2016; Kidd et al., 2011). Thus, when used as bait, MIP13 appears to function as a coactivator and brings in a factor(s) with transactivation activity. There were several interactions shown across MIPs. MIP11, a sorting nexin (Phan et al., 2008), interacted with the highest number of MIPs, including MIP2, MIP11, MIP12, MIP13, and MIP14 (Fig. 1). MIP3 is a MORC1 homolog, MORC6. The interaction between MORC1 and MORC6 was previously reported (Liu et al., 2014), and their heterodimer was shown to maintain heterochromatin compaction (Moissiard et al., 2012). Interestingly, MORC6 did not interact with any of the MIPs, suggesting that the MIPs are likely specific to MORC1.

***In planta* interactions of MORC1 with MIPs in *Nicotiana benthamiana*.** The MIP proteins were further examined to determine if the interaction occurs with MORC1 *in planta*. To this end, we transiently co-expressed MIPs and MORC1 tagged with HA and Myc, respectively, in *N. benthamiana*. The expressed proteins were subjected to a co-immunoprecipitation (co-IP) experiment in which an αHA antibody immunoprecipitated MIP proteins, and its co-IP of MORC1 was monitored by western analysis with an αMyc antibody. MIP4, MIP6, MIP7, MIP8, and MIP12 were not detectable via HA immunoblotting analysis (Fig. 2). MIP3 and MIP13 co-immunoprecipitated significantly more MORC1 than other weak interactors such as MIP9, MIP10, and MIP11 (Fig. 2). Note that MORC1 is known to be expressed as doublets, with the higher band suspected to result from post-translational modifications (Kang et al., 2012).

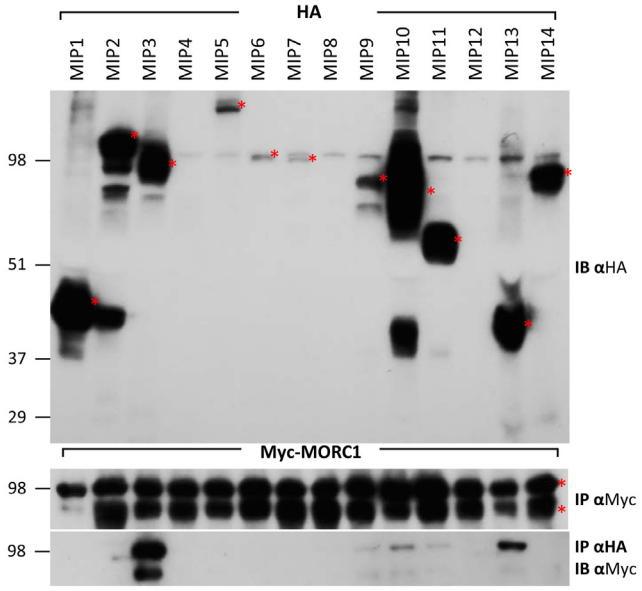

Fig. 2. Interaction of MORC1 with MORC1-interacting proteins (MIPs) *in planta*. Physical interaction of MORC1 and MIPs were tested in *Nicotiana benthamiana* plants transiently expressing *35S-Myc-MORC1* and *35S-HA-MIPs*. Proteins extracted were immunoprecipitated with anti-HA antibody. The asterisks indicate the expected sizes of MIP and MORC1 proteins. Expression of *Myc-MORC1* and *HA-MIPs* were examined by western analysis with anti-Myc and anti-HA antibodies, respectively. Co-immunoprecipitated proteins were detected by western analysis with anti-Myc antibody, indicating that MORC1 physically interacts with the MIPs in plant cells. IB, immunoblot; IP, immunoprecipitation.

Some MIPs are involved in bacterial resistance in Arabidopsis. Eight T-DNA insertion mutants for selected MIPs with annotated nuclear localization, similar to MORC1, were obtained from TAIR. We used an image-based resistance assay involving *Pst* carrying the luminescent *luxCDABE* reporter gene (Fan et al., 2008) to analyze the disease resistance phenotypes in a high-throughput manner. We used virulent *Pst* (*VirPst*) for infection, which provided the resistance phenotypes for basal resistance. *mip3*, *mip10*, and *mip13* were susceptible against *VirPst*, while *mip4* and *mip9* were resistant (Fig. 3). *mip8*, due to a homozygous lethality, was not further characterized.

***med9* mutant showed reduced resistance, but combining it with *morc1/2* restored resistance.** We showed that a knock-out mutant of MED9 displayed compromised resistance to *VirPst* (Fig. 3). As we have used an imaging-based assay, we suspected the magnitude of altered resistance could have been underestimated. Thus, we performed a conventional leaf-disc method to assess bacterial resistance

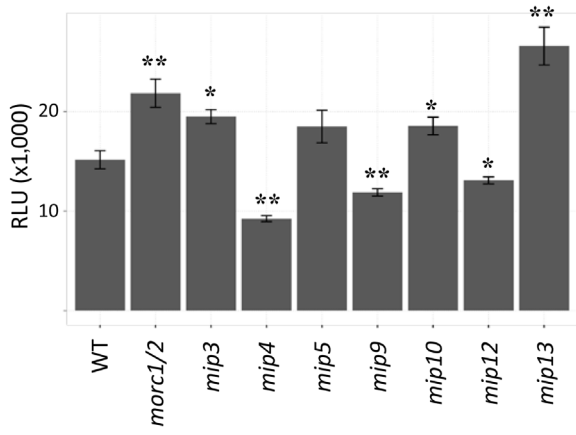

Fig. 3. Bacterial resistance of *mips* and *morc1/2* mutants against *Pseudomonas syringae* pv. *tomato* (*Pst*). Bacterial growth of *Pst* carrying a luminescent *luxCDABE* reporter gene was measured at 2 days post-inoculation (dpi) with the indicated genetic backgrounds; initial inoculum was at 1×10^5 cfu/ml. The luminescence was monitored by an electron-multiplying charge-coupled device (EMCCD) camera to indirectly measure the bacterial concentration. The mean ± standard error is presented ($n = 10$). Statistical difference from wild-type (WT) is indicated: $*P < 0.05$, $**P < 0.01$ (*t*-test).

in *med9*, *morc1/2*, and their higher-order mutant (*morc1/2 med9*).

The single mutants, *med9* and *morc1/2*, were susceptible to *VirPst* and avirulent *Pst* (*AvrPst*), suggesting that these components are involved in basal resistance and ETI. Unusually, *morc1/2 med9* regained WT-level resistance through an unknown mechanism (Fig. 4). Restoring resistance by combining two susceptible mutants is counterintuitive, which indicates that the MORC1 and MED9 interaction is likely multifaceted, perhaps involving various differential gene regulations over time. For instance, these factors may be essential in inducing defense genes early, while more engaged in curbing the induced genes later to minimize unnecessary fitness costs.

Transcriptional analysis of select defense genes to track defense signaling in MED9-associated genetic lines. We further characterized MED9 by tracking the expression of defense genes in *med9* and *morc1/2 med9* together with *morc1/2* in response to *AvrPst* and *VirPst* infection. We chose three well-characterized defense genes for our targeted transcriptional analysis: *PR1*, *PR2*, and *PR5* (Shah et al., 1997). Transcription dynamics of defense genes are also known to be an important predictor for successful resistance. For instance, *PR1* induction was delayed in *morc1/2* when examined at multiple time points (Bordiya et al.,

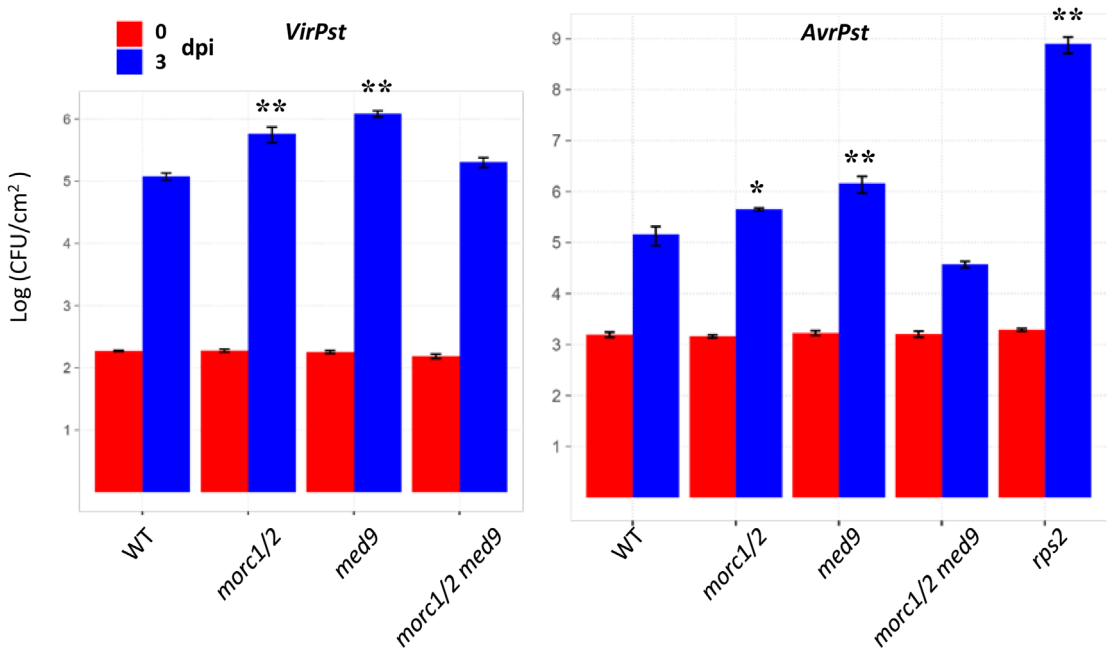

Fig. 4. Resistance phenotypes of *med9*, *morc1/2*, and *morc1/2 med9* mutants. Bacterial growth in the indicated plants was measured at 0 and 3 days post-inoculation (dpi) with virulent *Pseudomonas syringae* pv. *tomato* (*VirPst*) and *Pseudomonas syringae* pv. *tomato* carrying *AvrRpt2* (*AvrPst*). Initial inoculum of *VirPst* and *AvrPst* was at 1×10^5 and 5×10^5 cfu/ml, respectively; the mean ± standard deviation (n = 3) is presented. Statistical difference from wild-type (WT) is indicated: $*P < 0.05$, $**P < 0.01$ (*t*-test).

2016) which explains the susceptible resistance phenotype against *AvrPst* and *VirPst*. Thus, we decided to use the same multiple time points for our transcriptional analysis: 0, 1, 6, 24, and 48 hpi (hours post-infection).

qRT-PCR analysis was carried out for quantitative transcriptional analysis of *PR1*, *PR2*, and *PR5* in response to infection with *AvrPst* and *VirPst*; mock infection was used as a negative control. *PR1* was induced similarly in response to *AvrPst* among WT, *med9*, and *morc1/2* (Fig. 5A). However, the induction of *PR1* was slow (see 24 hpi with *AvrPst* in Fig. 5A) and trended upward even at 48 hpi in *morc1/2 med9*. This upward trend, while to a lesser degree, was seen with *PR2* and *PR5* at 48 hpi in *med9* and *morc1/2*. While it was less obvious than those responding to *AvrPst*, the induction rate of all the defense genes from 24 hpi to 48 hpi was steepest in *morc1/2 med9* responding to *VirPst*. Induction of *PR2* and *PR5* in *med9* and *morc1/2* was less robust and rapid relative to WT (Fig. 5B and C), consistent with their susceptible phenotypes to *AvrPst* and *VirPst*.

MED9 interaction with MORC1 occurred at later times in Arabidopsis. Physical MORC1-MED9 interaction was established in the Y2H assay (Fig. 1). As MORC1 displays nucleus-translocation in response to biotic stress (Kang et al., 2012), it is feasible that the MORC1-MED9 interaction depends on stress. To test this possibility, a transgenic Arabidopsis line carrying *Myc-MORC1* and *MED9-Flag* under their cognate promoters was subjected to a co-IP experiment, which confirmed physical interaction of the two proteins (Fig. 2). The MORC1-MED9 interaction was further investigated by monitoring levels of *PR1*, *PR2*, and *PR5* at 6 and 24 hpi with *AvrPst* treatments (Fig. 6) using co-IP, in which MORC1 was precipitated and MED9 was examined for co-IP. The results demonstrated that *AvrPst* significantly increased the MORC1-MED9 interaction at 24 hpi. In response to *AvrPst*, over 99% of the inducible defense genes in Arabidopsis peak at around 6 hpi and begin curbing this induced expression at 24 hpi (Mine et al., 2018). Note that three *PR* genes that display a 24-h peak are rather the exceptions than the rule in an overall group of genes showing a dynamic induction pattern (Mine et al., 2018). Given the kinetics of the defense gene induction, it is unlikely that MED9 interacts with MORC1 to enhance transcription. Instead, it is conceivable that MED9 interacts with MORC1 to restrain the overexpression of defense genes. Since MED14 interacts with a co-repressor LUG to facilitate target gene repression in Arabidopsis (Gonzalez et al., 2007), MED9 could also coordinate with MORC1 to repress defense genes at later time points.

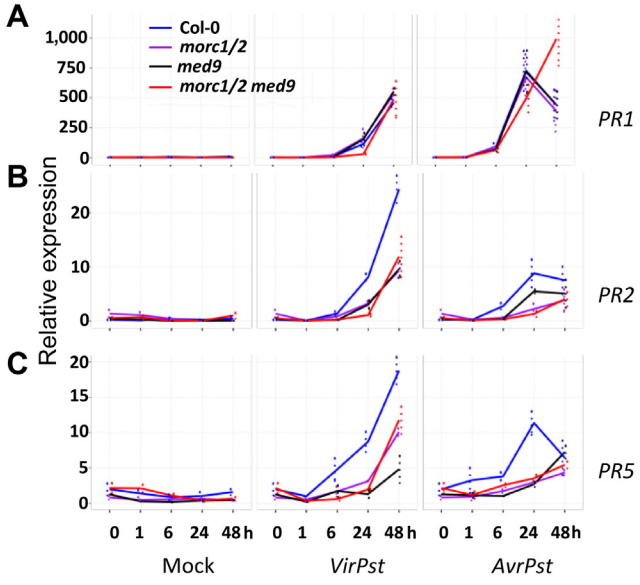

Fig. 5. MED9 regulates the expression of select defense genes in response to virulent *Pseudomonas syringae* pv. *tomato* (*VirPst*) and *Pseudomonas syringae* pv. *tomato* carrying *AvrRpt2* (*AvrPst*). Total RNA was isolated from 3.5-week-old plants of the indicated Arabidopsis lines that were infected with *VirPst*, *AvrPst*, or mock treatment at 1×10^6 cfu/ml for the indicated time points. Transcript levels were examined using real-time quantitative reverse transcription PCR with primers specific for *PR1* (A), *PR2* (B), and *PR5* (C). The *Tip41-like* gene was used as a reference gene for normalization. The mean ± standard error ($n = 6$) of two biological replicates is shown. Each biological replicate includes three technical replicates, with each dot representing one of these six technical replicates. 10 mM of $MgCl_2$ was used as mock treatment.

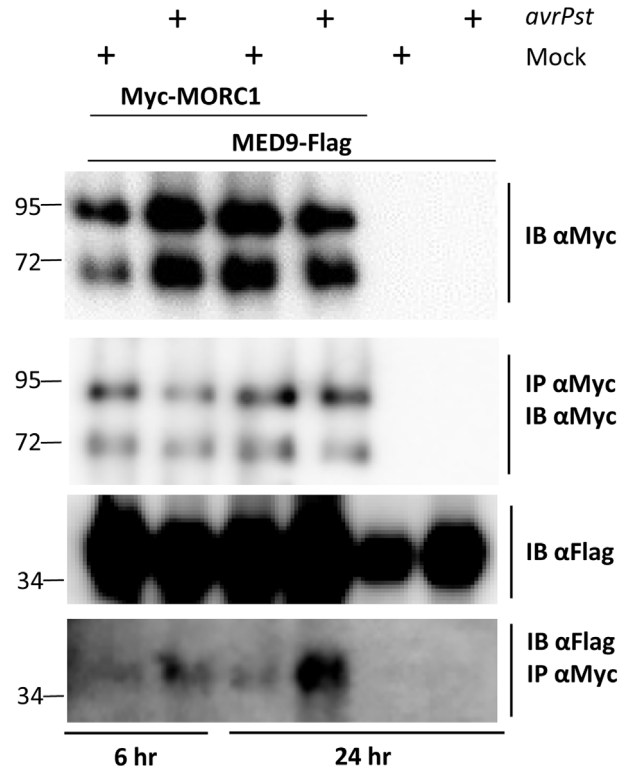

Fig. 6. Late interaction of MED9 with MORC1 during effector-triggered immunity. Three point five-week-old transgenic Arabidopsis line (first four lanes) carrying *Myc-MORC1* and *MED9-Flag* were used; both transgenes were under their native promoters. Plants were infected with *Pseudomonas syringae* pv. *tomato* carrying *AvrRpt2* (*AvrPst*) at 10^6 cfu/ml for the indicated times; a *MED9-Flag* transgeneic line was used as a negative control (the last two lanes). Proteins extracted were immunoprecipitated with anti-Myc antibody. Expression of *Myc-MORC1* and *MED9-Flag* was examined by immunoblot (IB) analysis with anti-Myc and anti-Flag antibodies, respectively. Proteins co-immunoprecipitated by anti-Myc antibody were detected by IB with anti-Myc and anti-Flag antibodies. IP, immunoprecipitation.

Fitness cost assessed by repeated pathogen challenges. We observed that *morc1/2* and *med9* displayed compromised resistance to *AvrPst* and *VirPst*, while *morc1/2 med9* regained WT-level resistance (Fig. 4). We further investigated this seemingly counterintuitive observation by tracking three commonly used defense genes (*PR1*, *PR2*, and *PR5*) to obtain a snapshot of defense signaling; this investigation revealed the slow but sustained expression of defense genes in *morc1/2 med9*. While regaining bacterial resistance to the level of WT through extended expression is likely beneficial to the host, it is frequently observed that excessive resistance incurs fitness-costs (Huot et al., 2014). Therefore, we hypothesized that regaining resistance in *morc1/2 med9* likely incurs a fitness-penalty.

We observed little difference in the morphology of *morc1/2*, *med9*, and *morc1/2 med9* at 3.5 weeks after germination relative to WT, as shown in the upper panel of Fig. 7A. These plants were then repeatedly infected with *AvrPst* at 1×10^5 cfu/ml every other day for 3 weeks and evaluated for their growth characteristics (Fig. 7B and C). First, the total weight was significantly reduced for *morc1/2 med9* when repeatedly challenged with *AvrPst* (Fig. 7B). We further characterized their growth and fertility characteristics: the weight and number of leaves, the weight and number of inflorescences, and the number of siliques (the long and narrow seedpods in Arabidopsis). Remarkably, only *morc1/2 med9* plants showed a significant reduction in all five measurements in response to *AvrPst* infection relative to the mock control (Fig. 7C), indicating a severe fitness cost incurred due to recurrent infection. For instance, the total leaf weight of *morc1/2 med9* was reduced

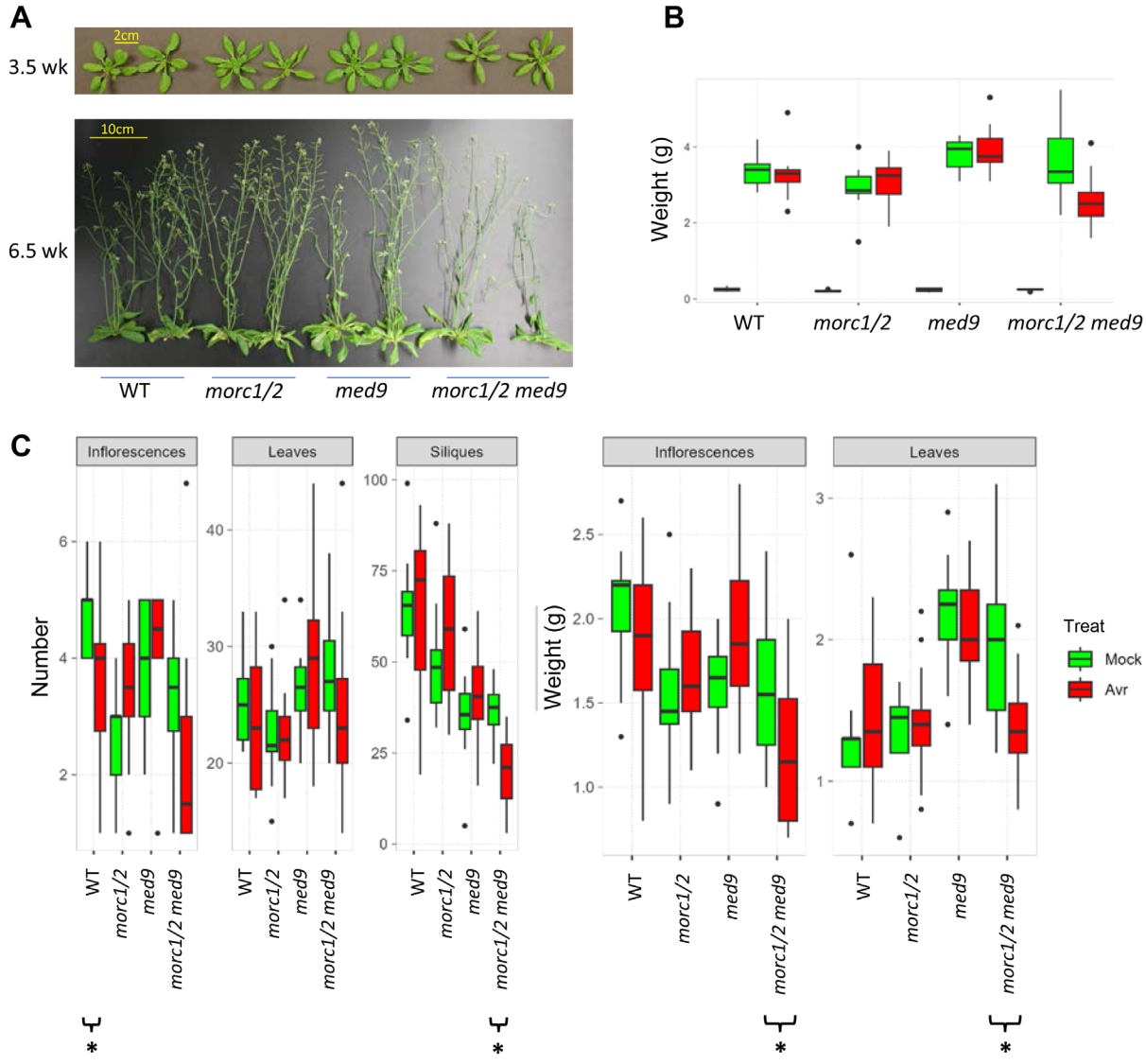

Fig. 7. Fitness cost assessment by repeated pathogen challenges. Three point five-week-old WT, *morc1/2*, *med9*, and *morc1/2 med9* were infected with *Pseudomonas syringae* pv. *tomato* carrying *AvrRpt2* (*AvrPst*) at 10^5 cfu/ml every 2 days for 3 weeks. (A) Representative plants before (upper) and after (lower) the repeated infection. (B) The weight of 3.5 weeks-old plants was measured. (C) Several growth and development characteristics were measured after the serial infection. To this end, the number of inflorescences, leaves, and siliques were counted, while the weight of inflorescences and leaves were measured. A minimum of ten plants in each line were examined. Statistical difference between mock and *AvrPst* treatment is indicated: *$P < 0.05$ (*t*-test).

by over 25% in response to *AvrPst* infection, while those of WT and the single mutants showed negligible changes. In particular, siliques of *morc1/2 med9* were significantly reduced in number, suggesting that sexual reproduction was also affected as a part of the fitness penalty.

Discussion

We identified 14 proteins interacting with MORC1 via Y2H screening, eight of which were predicted to be nuclear-localized and putative chromatin remodeling components. Among these, MED9, a member of the mediator complex that interfaces between transcription factors and RNA polymerase II (Samanta and Thakur, 2015a, 2015b), was identified. MED9 appears to be a positive regulator of plant defense signaling. Like MORC1, its loss led to compromised resistance to *Pst.*

Counterintuitively, a combined mutant, *morc1/2 med9* regained WT-level bacterial resistance, suggesting a complex genetic interaction, which are often reported. For example,

in a study on leaf sucrose content, the *mex1 phs1b* double mutant exhibited significantly lower levels compared to each respective single mutant, which showed higher levels than WT (Malinova et al., 2014). Similarly, while *nhx1* or *nhx2* single mutants develop flowers similar to or even longer than WT, the *nhx1 nhx2* double mutant, in contrast, exhibits shorter flower lengths (Bassil et al., 2011). These examples highlight the intricacy of genetic interactions and raise the question: how is *morc1/2 med9*, whose single mutants display compromised bacterial resistance, regaining WT-level resistance?

To address this question, we first measured the timing of the physical interaction between MORC1 and MED9 *in planta* and found the interaction enhanced at 24 hpi with *AvrPst*, not at 6 hpi. This later interaction suggests that the role of this interplay likely lies in later defense signaling (Fig. 6). A multi-point transcription study also indicates that induction of most defense genes under ETI peaks around 6 hpi, and most defense genes display downregulation by 24 hpi (Mine et al., 2018), suggesting that 24 hpi is likely a late time point for ETI. From this, we inferred that the MORC1-MED9 interaction functions to slow down the induced defense genes. In line with this inference, when we tracked the transcription dynamics of the defense genes at multiple time points responding to *AvrPst*, *morc1/2 med9* displayed sluggish but sustained expression of late defense genes, particularly *PR1*, that mainly peak at 24 hpi with *AvrPst*. This sustained expression pattern, which may explain how WT-level resistance was restored in *morc1/2 med9*, also pointed to the possibility that MORC1-MED9 interplay is important in late defense signaling, where transcriptional suppression becomes more dominant.

Heterochromatin is often associated with DNA methylation, and is typically marked by H3K9 methylation (H3K9me). In plants, the first identified H3K9 methyltransferase, KRYPTONITE (KYP)/SU(VAR)3–9 homolog 4 (SUVH4), functions partially redundantly with SUVH5 and SUVH6 to catalyze H3K9me (Ebbs and Bender, 2006; Jackson et al., 2002; Zhang et al., 2023). SUVH4/5/6 represses the expression of *R* genes and downstream defense-related genes, with the *suvh4 suvh5 suvh6* triple mutant exhibiting enhanced resistance to *Pst* (Cambiagno et al., 2021). IBM1, a major H3K9 demethylase in Arabidopsis, activates defense genes such as *PR1* and *PR2*, and *ibm1* mutants are hyper-susceptible to *Pst* (Chan and Zimmerli, 2019).

Given these observations, it is tempting to speculate that while MED9 mediates transcriptional activities, MORC1 could function to silence defense genes through chromatin compaction. This hypothesis is supported by the finding that *Caenorhabditis elegans* MORC1 compacts DNA (Kim et al., 2019). However, this idea seems counterintuitive, as MORC1 has been shown to be a positive regulator of ETI, with the loss of MORC1 and its homolog leading to the suppression of ETI (Kang et al., 2008, 2010). This suggests that MORC1 may have an additional function in early defense signaling that remains to be characterized.

The fitness cost of sustained *PR* gene expression and their associated defense signaling in *morc1/2 med9*, which resulted in restored WT-level resistance, became evident when the plants were repeatedly challenged with *AvrPst*. While there was little to no effect on those of WT, *med9*, and *morc1/2*, extended biotic stress triggered a significant reduction in the growth and reproduction of *morc1/2 med9* (Fig. 7), highlighting the importance of properly curbing defense signaling in time. Since fitness-costs of ETI were first reported in Arabidopsis (Tian et al., 2003), several signaling pathways have been reported to affect ETI-associated fitness costs (Richard et al., 2018). For instance, there is cross-talk and counter-regulation between the growth-related hormones including auxin, brassinosteroids, cytokinins, and gibberellins, and the defense-related ones including SA, ET, and JA (He et al., 2022). In addition, photosynthesis and its related genes are downregulated in response to *AvrPst* and *VirPst* (Bonfig et al., 2006). These growth-related components and their misregulation in response to bacterial infection could well be the reason why *morc1/2 med9* displayed notable fitness costs.

In this study, we identified 14 MIPs and characterized a genetic interaction between MED9 and MORC1. We found that sustained expression of the *PR* genes in *morc1/2 med9* restored resistance but incurred fitness penalties. This outcome may suggest that MORC1 is involved in down-regulating induced defense genes once immune responses are concluded, highlighting the importance of properly regulating biotic stress in a plant's fitness.

Conflicts of Interest

No potential conflict of interest relevant to this article was reported.

Acknowledgments

We thank Nicole Beisel for her assistance in constructing the clone, and to Angela Kang for reviewing the manuscript. This work was supported by the National Science Foundation (IOS-1553613, H.K).

References

Allen, B. L. and Taatjes, D. J. 2015. The Mediator complex: a central integrator of transcription. *Nat. Rev. Mol. Cell Biol*. 16:155-166.

An, C. and Mou, Z. 2013. The function of the Mediator complex in plant immunity. *Plant Signal. Behav*. 8:e23182.

Bassil, E., Tajima, H., Liang, Y.-C., Ohto, M.-A., Ushijima, K., Nakano, R., Esumi, T., Coku, A., Belmonte, M. and Blumwald, E. 2011. The *Arabidopsis* Na^+/H^+ antiporters NHX1 and NHX2 control vacuolar pH and K^+ homeostasis to regulate growth, flower development, and reproduction. *Plant Cell* 23:3482-3497.

Bonawitz, N. D., Kim, J. I., Tobimatsu, Y., Ciesielski, P. N., Anderson, N. A., Ximenes, E., Maeda, J., Ralph, J., Donohoe, B. S., Ladisch, M. and Chapple, C. 2014. Disruption of Mediator rescues the stunted growth of a lignin-deficient Arabidopsis mutant. *Nature* 509:376-380.

Bonfig, K. B., Schreiber, U., Gabler, A., Roitsch, T. and Berger, S. 2006. Infection with virulent and avirulent *P. syringae* strains differentially affects photosynthesis and sink metabolism in *Arabidopsis* leaves. *Planta* 225:1-12.

Bordiya, Y., Zheng, Y., Nam, J.-C., Bonnard, A. C., Choi, H. W., Lee, B.-K., Kim, J., Klessig, D. F., Fei, Z. and Kang, H.-G. 2016. Pathogen infection and MORC proteins affect chromatin accessibility of transposable elements and expression of their proximal genes in Arabidopsis. *Mol. Plant-Microbe Interact.* 29:674-687.

Boyer, L. A., Latek, R. R. and Peterson, C. L. 2004. The SANT domain: a unique histone-tail-binding module? *Nat. Rev. Mol. Cell Biol.* 5:158-163.

Brabbs, T. R., He, Z., Hogg, K., Kamenski, A., Li, Y., Paszkiewicz, K. H., Moore, K. A., O'Toole, P., Graham, I. A. and Jones, L. 2013. The stochastic silencing phenotype of Arabidopsis *morc6* mutants reveals a role in efficient RNA-directed DNA methylation. *Plant J*. 75:836-846.

Buendía-Monreal, M. and Gillmor, C. S. 2016. Mediator: a key regulator of plant development. *Dev. Biol.* 419:7-18.

Burdon, J. J. and Thrall, P. H. 2003. The fitness costs to plants of resistance to pathogens. *Genome Biol.* 4:227.

Caillaud, M.-C., Asai, S., Rallapalli, G., Piquerez, S., Fabro, G. and Jones, J. D. G. 2013. A downy mildew effector attenuates salicylic acid-triggered immunity in Arabidopsis by interacting with the host mediator complex. *PLoS Biol.* 11:e1001732.

Cambiagno, D. A., Torres, J. R. and Alvarez, M. E. 2021. Convergent epigenetic mechanisms avoid constitutive expression of immune receptor gene subsets. *Front. Plant Sci.* 12:703667.

Campos, M. L., Yoshida, Y., Major, I. T., de Oliveira Ferreira, D., Weraduwage, S. M., Froehlich, J. E., Johnson, B. F., Kramer, D. M., Jander, G., Sharkey, T. D. and Howe, G. A. 2016. Rewiring of jasmonate and phytochrome B signalling uncouples plant growth-defense tradeoffs. *Nat. Commun.* 7:12570.

Chan, C. and Zimmerli, L. 2019. The histone demethylase IBM1 positively regulates *Arabidopsis* immunity by control of defense gene expression. *Front. Plant Sci*. 10:1587.

Chen, R., Jiang, H., Li, L., Zhai, Q., Qi, L., Zhou, W., Liu, X., Li, H., Zheng, W., Sun, J. and Li, C. 2012. The *Arabidopsis* mediator subunit MED25 differentially regulates jasmonate and abscisic acid signaling through interacting with the MYC2 and ABI5 transcription factors. *Plant Cell* 24:2898-2916.

Chisholm, S. T., Coaker, G., Day, B. and Staskawicz, B. J. 2006. Host-microbe interactions: shaping the evolution of the plant immune response. *Cell* 124:803-814.

Conaway, R. C. and Conaway, J. W. 2011. Origins and activity of the Mediator complex. *Semin. Cell Dev. Biol*. 22:729-734.

Davière, J.-M. and Achard, P. 2013. Gibberellin signaling in plants. *Development* 140:1147-1151.

Dempsey, D. A., Pathirana, M. S., Wobbe, K. K. and Klessig, D. F. 1997. Identification of an *Arabidopsis* locus required for resistance to turnip crinkle virus. *Plant J.* 11:301-311.

Dhawan, R., Luo, H., Foerster, A. M., Abuqamar, S., Du, H.-N., Briggs, S. D., Mittelsten Scheid, O. and Mengiste, T. 2009. HISTONE MONOUBIQUITINATION1 interacts with a subunit of the mediator complex and regulates defense against necrotrophic fungal pathogens in *Arabidopsis. Plant Cell* 21:1000-1019.

Dröge-Laser, W., Snoek, B. L., Snel, B. and Weiste, C. 2018. The Arabidopsis bZIP transcription factor family: an update. *Curr. Opin. Plant Biol.* 45:36-49.

Ebbs, M. L. and Bender, J. 2006. Locus-specific control of DNA methylation by the *Arabidopsis* SUVH5 histone methyltransferase. *Plant Cell* 18:1166-1176.

Fallath, T., Kidd, B. N., Stiller, J., Davoine, C., Björklund, S., Manners, J. M., Kazan, K. and Schenk, P. M. 2017. *MEDIATOR18* and *MEDIATOR20* confer susceptibility to *Fusarium oxysporum* in *Arabidopsis thaliana*. *PLoS ONE* 12:e0176022.

Fan, J., Crooks, C. and Lamb, C. 2008. High-throughput quantitative luminescence assay of the growth in planta of *Pseudomonas syringae* chromosomally tagged with *Photorhabdus luminescens luxCDABE*. *Plant J*. 53:393-399.

Gangappa, S. N., Berriri, S. and Kumar, S. V. 2017. PIF4 coordinates thermosensory growth and immunity in *Arabidopsis*. *Curr. Biol*. 27:243-249.

Gieni, R. S. and Hendzel, M. J. 2009. Actin dynamics and functions in the interphase nucleus: moving toward an understanding of nuclear polymeric actin. *Biochem. Cell Biol.* 87:283-306.

Gonzalez, D., Bowen, A. J., Carroll, T. S. and Conlan, R. S. 2007. The transcription corepressor LEUNIG interacts with the histone deacetylase HDA19 and mediator components MED14 (SWP) and CDK8 (HEN3) to repress transcription. *Mol. Cell. Biol*. 27:5306-5315.

Hammond-Kosack, K. E. and Jones, J. D. 1996. Resistance gene-dependent plant defense responses. *Plant Cell* 8:1773-1791.

He, Z., Webster, S. and He, S. Y. 2022. Growth-defense trade-offs in plants. *Curr. Biol*. 32:R634-R639.

Hoppmann, V., Thorstensen, T., Kristiansen, P. E., Veiseth, S.

V., Rahman, M. A., Finne, K., Aalen, R. B. and Aasland, R. 2011. The CW domain, a new histone recognition module in chromatin proteins. *EMBO J.* 30:1939-1952.

Huot, B., Yao, J., Montgomery, B. L. and He, S. Y. 2014. Growth-defense tradeoffs in plants: a balancing act to optimize fitness. *Mol. Plant* 7:1267-1287.

Iyer, L. M., Abhiman, S. and Aravind, L. 2008. MutL homologs in restriction-modification systems and the origin of eukaryotic MORC ATPases. *Biol. Direct* 3:8.

Jackson, J. P., Lindroth, A. M., Cao, X. and Jacobsen, S. E. 2002. Control of CpNpG DNA methylation by the KRYPTONITE histone H3 methyltransferase. *Nature* 416:556-560.

Jones, J. D. G. and Dangl, J. L. 2006. The plant immune system. *Nature* 444:323-329.

Kang, H.-G., Choi, H. W., von Einem, S., Manosalva, P., Ehlers, K., Liu, P.-P., Buxa, S. V., Moreau, M., Mang, H.-G., Kachroo, P., Kogel, K.-H. and Klessig, D. F. 2012. CRT1 is a nuclear-translocated MORC endonuclease that participates in multiple levels of plant immunity. *Nat. Commun*. 3:1297.

Kang, H.-G. and Klessig, D. F. 2005. Salicylic acid-inducible *Arabidopsis* CK2-like activity phosphorylates TGA2. *Plant Mol. Biol*. 57:541-557.

Kang, H.-G., Kuhl, J. C., Kachroo, P. and Klessig, D. F. 2008. CRT1, an Arabidopsis ATPase that interacts with diverse resistance proteins and modulates disease resistance to turnip crinkle virus. *Cell Host Microbe* 3:48-57.

Kang, H.-G., Oh, C.-S., Sato, M., Katagiri, F., Glazebrook, J., Takahashi, H., Kachroo, P., Martin, G. B. and Klessig, D. F. 2010. Endosome-associated CRT1 functions early in resistance gene-mediated defense signaling in *Arabidopsis* and tobacco. *Plant Cell* 22:918-936.

Karasov, T. L., Chae, E., Herman, J. J. and Bergelson, J. 2017. Mechanisms to mitigate the trade-off between growth and defense. *Plant Cell* 29:666-680.

Kelleher, R. J. 3rd, Flanagan, P. M. and Kornberg, R. D. 1990. A novel mediator between activator proteins and the RNA polymerase II transcription apparatus. *Cell* 61:1209-1215.

Kidd, B. N., Cahill, D. M., Manners, J. M., Schenk, P. M. and Kazan, K. 2011. Diverse roles of the Mediator complex in plants. *Semin. Cell Dev. Biol*. 22:741-748.

Kidd, B. N., Edgar, C. I., Kumar, K. K., Aitken, E. A., Schenk, P. M., Manners, J. M. and Kazan, K. 2009. The mediator complex subunit PFT1 is a key regulator of jasmonate-dependent defense in *Arabidopsis*. *Plant Cell* 21:2237-2252.

Kim, H., Yen, L., Wongpalee, S. P., Kirshner, J. A., Mehta, N., Xue, Y., Johnston, J. B., Burlingame, A. L., Kim, J. K., Loparo, J. J. and Jacobsen, S. E. 2019. The gene-silencing protein MORC-1 topologically entraps DNA and forms multimeric assemblies to cause DNA compaction. *Mol. Cell* 75:700-710.

Koch, A., Kang, H.-G., Steinbrenner, J., Dempsey, D. A., Klessig, D. F. and Kogel, K.-H. 2017. MORC proteins: novel players in plant and animal health. *Front. Plant Sci*. 8:1720.

Li, F., Cheng, C., Cui, F., de Oliveira, M. V., Yu, X., Meng, X., Intorne, A. C., Babilonia, K., Li, M., Li, B., Chen, S., Ma, X., Xiao, S., Zheng, Y., Fei, Z., Metz, R. P., Johnson, C. D., Koiwa, H., Sun, W., Li, Z., de Souza Filho, G. A., Shan, L. and He, P. 2014. Modulation of RNA polymerase II phosphorylation downstream of pathogen perception orchestrates plant immunity. *Cell Host Microbe* 16:748-758.

Liu, Z.-W., Shao, C.-R., Zhang, C.-J., Zhou, J.-X., Zhang, S.-W., Li, L., Chen, S., Huang, H.-W., Cai, T. and He, X.-J. 2014. The SET domain proteins SUVH2 and SUVH9 are required for Pol V occupancy at RNA-directed DNA methylation loci. *PLoS Genet*. 10:e1003948.

Lorkovic, Z. J., Naumann, U., Matzke, A. J. M. and Matzke, M. 2012. Involvement of a GHKL ATPase in RNA-directed DNA methylation in *Arabidopsis thaliana*. *Curr. Biol*. 22:933-938.

Malik, N., Agarwal, P. and Tyagi, A. 2017. Emerging functions of multi-protein complex Mediator with special emphasis on plants. *Crit. Rev. Biochem. Mol. Biol*. 52:475-502.

Malinova, I., Mahlow, S., Alseekh, S., Orawetz, T., Fernie, A. R., Baumann, O., Steup, M. and Fettke, J. 2014. Double knockout mutants of Arabidopsis grown under normal conditions reveal that the plastidial phosphorylase isozyme participates in transitory starch metabolism. *Plant Physiol*. 164:907-921.

Menke, F. L. H., Kang, H.-G., Chen, Z., Park, J. M., Kumar, D. and Klessig, D. F. 2005. Tobacco transcription factor WRKY1 is phosphorylated by the MAP kinase SIPK and mediates HR-like cell death in tobacco. *Mol. Plant-Microbe Interact*. 18:1027-1034.

Mine, A., Seyfferth, C., Kracher, B., Berens, M. L., Becker, D. and Tsuda, K. 2018. The defense phytohormone signaling network enables rapid, high-amplitude transcriptional reprogramming during effector-triggered immunity. *Plant Cell* 30:1199-1219.

Moissiard, G., Bischof, S., Husmann, D., Pastor, W. A., Hale, C. J., Yen, L., Stroud, H., Papikian, A., Vashisht, A. A., Wohlschlegel, J. A. and Jacobsen, S. E. 2014. Transcriptional gene silencing by Arabidopsis microrchidia homologues involves the formation of heteromers. *Proc. Natl. Acad. Sci. U. S. A.* 111:7474-7479.

Moissiard, G., Cokus, S. J., Cary, J., Feng, S., Billi, A. C., Stroud, H., Husmann, D., Zhan, Y., Lajoie, B. R., McCord, R. P., Hale, C. J., Feng, W., Michaels, S. D., Frand, A. R., Pellegrini, M., Dekker, J., Kim, J. K. and Jacobsen, S. E. 2012. MORC family ATPases required for heterochromatin condensation and gene silencing. *Science* 336:1448-1451.

Navarro, L., Bari, R., Achard, P., Lisón, P., Nemri, A., Harberd, N. P. and Jones, J. D. G. 2008. DELLAs control plant immune responses by modulating the balance of jasmonic acid and salicylic acid signaling. *Curr. Biol*. 18:650-655.

Ngou, B. P. M., Ahn, H.-K., Ding, P. and Jones, J. D. G. 2021. Mutual potentiation of plant immunity by cell-surface and intracellular receptors. *Nature* 592:110-115.

Nicolau, M., Picault, N., Descombin, J., Jami-Alahmadi, Y., Feng, S., Bucher, E., Jacobsen, S. E., Deragon, J.-M., Wohlschlegel, J. and Moissiard, G. 2020. The plant mobile domain proteins

MAIN and MAIL1 interact with the phosphatase PP7L to regulate gene expression and silence transposable elements in *Arabidopsis thaliana*. *PLoS Genet.* 16:e1008324.

Phan, N. Q., Kim, S.-J. and Bassham, D. C. 2008. Overexpression of *Arabidopsis* sorting nexin AtSNX2b inhibits endocytic trafficking to the vacuole. *Mol. Plant* 1:961-976.

Pujara, D. S., Kim, S.-I., Nam, J. C., Mayorga, J., Elmore, I., Kumar, M., Koiwa, H. and Kang, H.-G. 2021. Imaging-based resistance assay using enhanced luminescence-tagged *Pseudomonas syringae* reveals a complex epigenetic network in plant defense signaling pathways. *Mol. Plant-Microbe Interact*. 34:990-1000.

Richard, M. M. S., Gratias, A., Meyers, B. C. and Geffroy, V. 2018. Molecular mechanisms that limit the costs of NLR-mediated resistance in plants. *Mol. Plant Pathol*. 19:2516-2523.

Samanta, S. and Thakur, J. K. 2015a. Importance of Mediator complex in the regulation and integration of diverse signaling pathways in plants. *Front. Plant Sci*. 6:757.

Samanta, S. and Thakur, J. K. 2015b. Role of plant mediator complex in stress response. In: *Elucidation of abiotic stress signaling in plants: functional genomics perspectives*, ed. by G. K. Pandey, Vol. 2, pp. 3-28. Springer, New York, NY, USA.

Shah, J., Tsui, F. and Klessig, D. F. 1997. Characterization of a salicylic acid-insensitive mutant (*sai1*) of *Arabidopsis thaliana*, identified in a selective screen utilizing the SA-inducible expression of the *tms2* gene. *Mol. Plant-Microbe Interact*. 10:69-78.

Sun, J., Chen, Q., Qi, L., Jiang, H., Li, S., Xu, Y., Liu, F., Zhou, W., Pan, J., Li, X., Palme, K. and Li, C. 2011. Jasmonate modulates endocytosis and plasma membrane accumulation of the Arabidopsis PIN2 protein. *New Phytol*. 191:360-375.

Tao, Y., Xie, Z., Chen, W., Glazebrook, J., Chang, H.-S., Han, B., Zhu, T., Zou, G. and Katagiri, F. 2003. Quantitative nature of Arabidopsis responses during compatible and incompatible interactions with the bacterial pathogen *Pseudomonas syringae*. *Plant Cell* 15:317-330.

Tian, D., Traw, M. B., Chen, J. Q., Kreitman, M. and Bergelson, J. 2003. Fitness costs of R-gene-mediated resistance in *Arabidopsis thaliana*. *Nature* 423:74-77.

Tsuda, K., Sato, M., Stoddard, T., Glazebrook, J. and Katagiri, F. 2009. Network properties of robust immunity in plants. *PLoS Genet*. 5:e1000772.

van Hulten, M., Pelser, M., van Loon, L. C., Pieterse, C. M. J. and Ton, J. 2006. Costs and benefits of priming for defense in *Arabidopsis*. *Proc. Natl. Acad. Sci. U. S. A*. 103:5602-5607.

Wang, C., Yao, J., Du, X., Zhang, Y., Sun, Y., Rollins, J. A. and Mou, Z. 2015. The Arabidopsis mediator complex subunit16 is a key component of basal resistance against the necrotrophic fungal pathogen *Sclerotinia sclerotiorum*. *Plant Physiol*. 169:856-872.

Wood, A. J., Severson, A. F. and Meyer, B. J. 2010. Condensin and cohesin complexity: the expanding repertoire of functions. *Nat. Rev. Genet.* 11:391-404.

Yang, Y., Li, L. and Qu, L.-J. 2016. Plant mediator complex and its critical functions in transcription regulation. *J. Integr. Plant Biol*. 58:106-118.

Zhang, J., Yuan, J., Lin, J., Chen, L., You, L.-Y., Chen, S., Peng, L., Wang, C.-H., Du, J. and Duan, C.-G. 2023. Molecular basis of locus-specific H3K9 methylation catalyzed by SUVH6 in plants. *Proc. Natl. Acad. Sci. U. S. A.* 120:e2211155120.

Zhang, X., Wang, C., Zhang, Y., Sun, Y. and Mou, Z. 2012. The *Arabidopsis* mediator complex subunit16 positively regulates salicylate-mediated systemic acquired resistance and jasmonate/ethylene-induced defense pathways. *Plant Cell* 24:4294-4309.

Zhang, X., Yao, J., Zhang, Y., Sun, Y. and Mou, Z. 2013. The Arabidopsis Mediator complex subunits MED14/SWP and MED16/SFR6/IEN1 differentially regulate defense gene expression in plant immune responses. *Plant J*. 75:484-497.

Zhu, X., Zhang, Y., Bjornsdottir, G., Liu, Z., Quan, A., Costanzo, M., López, M. D., Westholm, J. O., Ronne, H., Boone, C., Gustafsson, C. M. and Myers, L. C. 2011. Histone modifications influence mediator interactions with chromatin. *Nucleic Acids Res.* 39:8342-8354.

Zipfel, C. and Felix, G. 2005. Plants and animals: a different taste for microbes? *Curr. Opin. Plant Biol*. 8:353-360.